OPTIMIZATION OF DIPOLE-FIELD PROFILES FOR EMITTANCE REDUCTION IN STORAGE RINGS*

C.-x. Wang†, Y. Wang, ANL, Argonne, IL 60439, USA
Y. Peng, IHEP, Beijing, 100049, China

Abstract

Nonuniform dipoles with bending field variation have been studied for reducing storage ring emittance in recent years. According to a new minimum emittance theory, the effects of an arbitrary dipole can be characterized by two parameters. To have a better idea of the potentials of nonuniform dipoles, here we numerically explore the values of these two parameters for optimal emittance reduction.

INTRODUCTION

Minimizing beam emittance in storage rings is desired by ever-increasing demands of higher beam quality for both modern synchrotron light sources and damping rings in high-energy linear colliders. In recent years, there have been efforts to reduce the emittance below the well-known theoretical minimum by using dipoles with bending-radius variation [1-5] The new theoretical minimum emittance with arbitrary dipoles was established [5] as

$$\epsilon = \frac{C_q \gamma^2}{J_x} \mathcal{F}^{\min}, \tag{1}$$

where $C_q = 3.84 \times 10^{-13}$ m; γ is the Lorentz factor; and J_x is the horizontal damping partition number, which we will not consider here. The lattice-dependent factor $\mathcal{F}$ is given for three types of commonly interested lattices: AME stands for the minimum emittance under achromatic conditions, and TME and EME stand for the theoretical minimum emittance and effective minimum emittance, respectively. The minimal $\mathcal{F}$ for these lattices reads

$$\mathcal{F}^{\min} = 2\sqrt{|A|} \begin{cases} 1 & \text{AME} \\ \sqrt{1-c} & \text{TME} \\ \sqrt{\frac{[1+(q+3)\,qc/2]\,[1+((1+\tau)q+3)\,qc/2]}{1+qc}}, & \text{EME} \end{cases} \tag{2}$$

where $|A|$ and c are two parameters solely determined by the dipole; $\tau = J_x/J_E$ is the ratio of horizontal to longitudinal damping partition numbers; and the q parameter is determined by the cubic equation

$$(1+\tau)q^3 + 2(2+\tau)q^2 + [3 + (2+\tau)/c]q + 2/c = 0. \tag{3}$$

In this paper, we will use the nominal value $\tau = 1/2$, while the effect of changing τ has been addressed in [5].

* Work supported by U.S. Department of Energy, Office of Science, Office of Basic Energy Sciences, under Contract No. DE-AC02-06CH11357.

† wangcx@aps.anl.gov

Developed from the general minimum emittance theory, the $|A|$ and c parameters are characteristics of a dipole magnet. For typical uniform dipoles of bending angle θ, $2\sqrt{|A|} \simeq \theta^3/4\sqrt{15}$ and $c \simeq 8/9$ under the usually good small-angle approximation. It has been shown that it is possible to reduce $|A|$ and increase c, thus reducing minimum emittance, by optimizing the bending radius profile of dipole magnets. It also becomes clear that the minimum emittance can approach zero mathematically, except for practical limitations due to magnetic field strength and so on. Thus, a natural question is the potential gains in emittance reduction that nonuniform dipoles may provide. A clear and easy answer is practically important in order for machine designers to decide whether it is worthwhile to explore such a potential. The fact that an arbitrary dipole can be characterized by only two values $|A|$ and c (thus a single point in $|A|$-c parameter space instead of a detailed bending-radius profile) provides an effective way to investigate and present a clear picture of the potentials of nonuniform dipoles for emittance reduction. In other words, the answer to the question lies in the distribution of dipoles in the $|A|$-c parameter space, especially the distribution of optimized dipole-field profiles and corresponding emittances. This paper reports an optimization study of dipole-field profiles using genetic-algorithm (GA)-based optimizers.

Since there are two objective parameters to optimize, we choose to compute the Pareto-optimal solutions in the $|A|$-c parameter space using a multi-objective GA optimizer based on the NSGA-II algorithm [6]. For convenience, we adopted a Mathematica™ implementation of this algorithm [7]. As an independent check and further refinement, a single-objective parallel GA package [8] is also used to optimize some special cases. Good agreements are found for comparable results.

In the following sections, we will briefly describe the methods used for this study, and then present some of our results in graphs that hopefully give a clear picture of the potentials to reduce beam emittance with nonuniform dipoles. A more complete presentation will be published soon.

METHODS

To evaluate the efficacy of nonuniform dipoles for emittance reduction as well as lattice feasibility, we use as the reference a uniform dipole, 1 meter long with 10-meter bending radius, and compare it with nonuniform dipoles having the same length and bending angle. The resulting emittance reduction factor and the ratio of initial lattice functions should apply to other dipole parameters, as long as the small-angle approximation is valid, thanks to the scale-invariant property of the theory. This helps to reduce the complexity of the problem dramatically and makes our optimization results suitable as a general reference for the potentials of nonuniform dipoles.

To optimize a field profile, we use a large number (33 for the results presented here) of equal-length dipole slices to approximate an arbitrary dipole and use the bending curvature $h(s) = 1/\rho(s)$ to represent a dipole-field profile, where $\rho(s)$ is the bending radius. Our computation starts from the basic quantity in the minimum emittance theory, i.e., the projected dispersion vector $\hat{\boldsymbol{\xi}} = [\hat{\xi}, \hat{\xi}']^T$ that relates to the dispersion vector $\boldsymbol{\eta}$ via $\boldsymbol{\eta}(s) = M(s)\left(\boldsymbol{\eta}_0 + \hat{\boldsymbol{\xi}}(s)\right)$, where M is the linear transfer matrix and $\boldsymbol{\eta}_0$ is the initial dispersion. To numerically solve for the projected dispersion $\hat{\xi}$ and $\hat{\xi}_p \equiv \hat{\xi}'$, we directly solve the first-order differential equations $\hat{\boldsymbol{\xi}}' = M^{-1}[0, h]^T$, i.e., $\hat{\xi}' = -hM_{12}$ and $\hat{\xi}_p' = hM_{11}$ with the initial conditions $\hat{\xi}(0) = \hat{\xi}_p(0) = 0$. Using $\hat{\boldsymbol{\xi}}$ we can compute the matrices A, B, and the parameter c as defined by

$$A = \langle\!\langle \hat{\boldsymbol{\xi}}\hat{\boldsymbol{\xi}}^T \rangle\!\rangle, \quad B = \frac{\langle\!\langle \hat{\boldsymbol{\xi}} \rangle\!\rangle \langle\!\langle \hat{\boldsymbol{\xi}} \rangle\!\rangle^T}{\check{\rho}}, \quad \text{and} \quad c = -\frac{\mathrm{Tr}(JAJB)}{|A|}, \tag{4}$$

where $\langle\!\langle v \rangle\!\rangle \equiv \langle v|h|^3\rangle / \langle h^2 \rangle$, $\check{\rho} \equiv \langle\!\langle 1 \rangle\!\rangle$, and $J = [0, 1; -1, 0]$. The average over the dipole, $\langle \cdot\cdot \rangle$, is done by numerical integration.

The optimization is carried out with GA optimizers. A population of 100 individuals is randomly initialized with each individual having a chromosome length equal to the number of dipole slices. The population is then evolved using the elitist multi-objective optimizer based on genetic algorithm with non-dominated sorting (NSGA-II). After sufficient generations, the Pareto-optimal solutions are obtained. The emittance and optimal lattice parameters are computed for each individual in the optimal solutions and the results are summarized in graphs. As an independent check and for better converging efficiency, a single-objective parallel GA package (PGApack) is used to optimize the AME, TME, and EME emittances directly, which should reproduce the corresponding extreme points of emittance curves obtained from the optimal population.

To estimate lattice feasibility of an optimal solution, we compute the ratio of initial lattice parameters of the optimized profile to the reference uniform dipole. Such information should indicate the difficulty of realizing an optimized result, although it is much more involved to design a lattice. The lattice-parameter distribution on the Pareto-optimal solutions provides a useful way to make a trade-off between emittance reduction and lattice difficulty. Our goal is to understand the landscape for emittance reduction.

OPTIMIZATION RESULTS

Pareto-Optimal Solutions

Pareto-optimal solutions in the objective space reveal compromises among multiple objectives to be optimized.

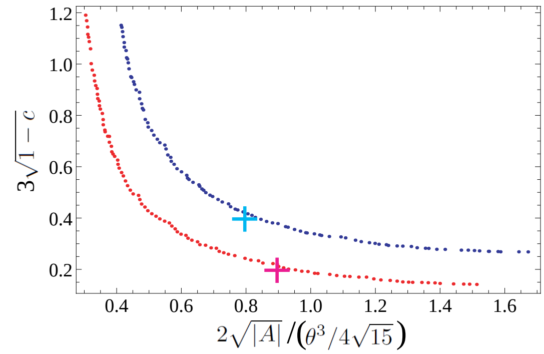

Figure 1: Pareto-optimal solutions in the objective space. The colored dots represent a population of 100 whose maximum field strength is higher than the reference dipole by a factor of 2 (blue) and 4 (red). The markers represent results of single-objective PGA optimization of TME.

In our case, we need to minimize $|A|$ and maximize c for minimal emittance. In fact, we choose to minimize both $2\sqrt{|A|}$ and $\sqrt{1-c}$, normalized by the values of the reference uniform dipole. The resulting Pareto-optimal solutions under several maximum field strengths are plotted in Fig. 1. From this information and the emittance formula, it is easy to see the potential emittance reduction using nonuniform dipoles. To be more explicit, we computed the emittance reduction factor for AME, TME, and EME lattices using the optimal solutions in Fig. 1 and summarized the results in Fig. 2. The behaviors of AME and EME are similar, and both are dominated by the $2\sqrt{|A|}$ factor. This is good since both AME and EME are of interest to light sources, and the similarity may allow some flexibility in switching lattices. On the other hand, the TME reduction is much larger and dominated by the $\sqrt{1-c}$ factor. This plot suggests that nonuniform dipoles will be more effective for damping rings since they favor TME lattices. Note

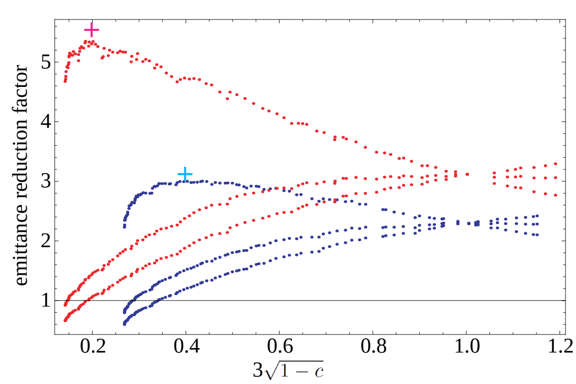

Figure 2: Emittance reduction factors for AME, TME, and EME lattices at maximum field strength 2 (blue) and 4 (red) times higher. The markers represent results of single-objective PGA optimization of TME, which show good agreement, although the multi-objective optimization is yet to converge to the optimal.

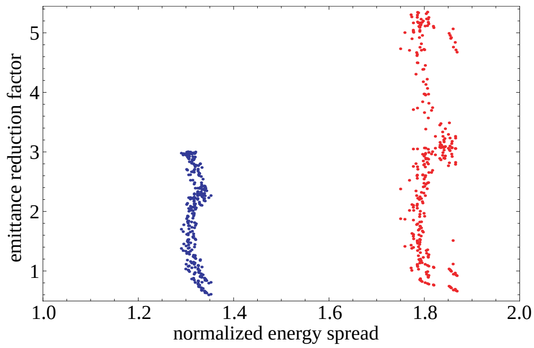

Figure 3: Relative increases in beam energy spread for the optimal solutions.

that dipoles optimized for TME are not effective at all for AME and EME. To show the relative increase in beam energy spread, Fig. 3 plots the AME, TME, and EME versus the energy spread for the two sets of Pareto-optimal solutions. The increase in energy spread might limit the usefulness of nonuniform dipoles in some machines.

Lattice Parameters for Optimal Emittance

In order to get some idea of the difficulty in implementing lattices of the optimal solutions, Fig. 4 plots the emittances versus the relative change in initial beta functions. It is encouraging to see that significant emittance reduction (not far from the optimum) can be achieved without large changes in the initial Twiss parameters. Furthermore, Fig. 5 plots the relative change in initial beta functions versus the initial alpha functions. It shows that the changes in beta and alpha functions are more or less proportional, which indicates that the emittance reduction is less sensitive to deviations in initial Twiss parameters (see Fig. 1 in [5]). Due to space limitations, we will leave other factors such as dispersion functions to a future publication.

Field Profiles

The optimal bending curvatures for a couple of special cases are shown in Fig. 6. Note that emittance reduction is

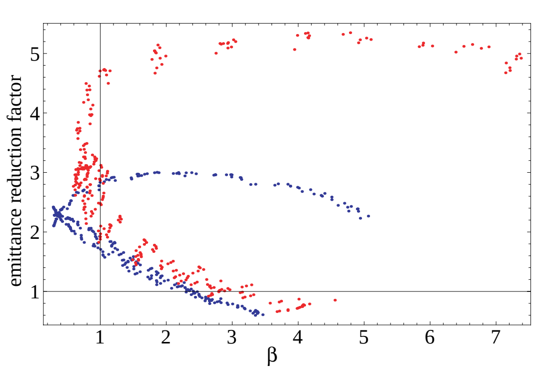

Figure 4: Relative changes in initial β functions for the optimal solutions.

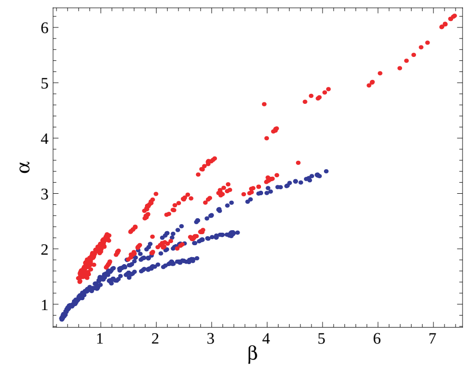

Figure 5: Relative changes in initial β and α functions for the optimal solutions.

not very sensitive to field errors.

Thanks M. Borland and Q. Qin for introducing Y. Wang and Y. Peng, respectively, to work on this subject. Thanks to L. Emery for support and helpful discussions.

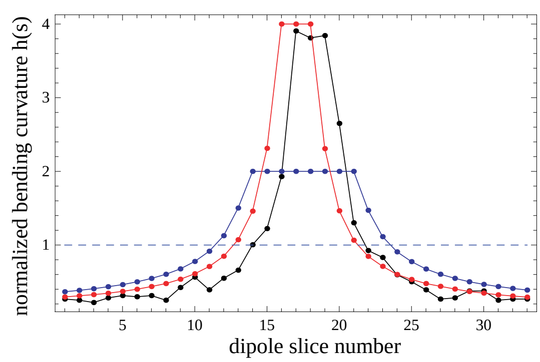

Figure 6: Optimal curvature profiles (from PGA) for minimal TME at maximum field strength 2 (blue) and 4 (red) times higher than the reference dipole (dash). The black one is from multi-objective optimization, which is not fully optimized, with a few percentage lower performance.

REFERENCES

[1] J. Guo and T. Raubenheimer, EPAC'02, Paris, June 2002, p. 1136 (2002).

[2] Y. Papaphilippou, P. Elleaume, PAC'05, Knoxville, May 2005, p. 2086 (2005).

[3] R. Nagaoka, A.F. Wrulich, NIM A575, 292 (2007).

[4] A. Streun, PSI Internal Report SLS-TME-TA-2006-0297 (2007).

[5] C.-x. Wang, Phys. Rev. ST-AB **12**, 061001 (2009).

[6] K. Deb, A. Pratap, S. Agarwal, and T. Meyarivan, IEEE TEC **6**(2), 182 (2002).

[7] R. Gruna, "Evolutionary Multiobjective Optimization" from The Wolfram Demonstration Project `http://demonstrations.wolfram.com/EvolutionaryMultiobjectiveOptimization`.

[8] D. Levine, ANL-95/18 (1996).